Journal of The Electrochemical Society, **158** (12) C416-C423 (2011)
0013-4651/2011/158(12)/C416/8/$28.00 © The Electrochemical Society

Electrosynthesis of PANI-Nano TiO_2 Composite Coating on Steel and Its Anti-Corrosion Performance

V. Karpakam, K. Kamaraj, and S. Sathiyanarayanan[z]

CSIR-Central Electrochemical Research Institute, Karaikudi-630006, India

PANI-nano TiO_2 composite coatings on a steel electrode have been successfully electrosynthesized from aniline in aqueous oxalic acid solution containing nano TiO_2 using cyclic voltammetry. Formation of the PANI-TiO_2 coating was found to be strongly dependent on the number of cycles. Smooth and strongly adherent PANI-TiO_2 coatings were obtained during sequential scanning of the potential region between −0.5 to 1.6 V, at a scan rate of 10 mV s^{-1}. During the repetitive cyclic voltammetry scans the presence of TiO_2 nanoparticles inhibits the polymer oxidation process. Good adhesion of composite coatings on the steel electrode, with superior electro-active characteristics in comparison with pure polyaniline, was demonstrated. PANI-TiO_2 coatings were characterized by FT-IR, SEM, and XPS techniques. The corrosion behaviour of coated steel was investigated by Electrochemical Impedance Spectroscopy and Tafel studies in 1 % NaCl solution and it was found that the PANI-TiO_2 coating was found to be more corrosion resistant than that of pure PANI coating due to compact coating formation.
 [DOI: 10.1149/2.023112jes]

Manuscript submitted July 26, 2011; revised manuscript received August 30, 2011. Published October 31, 2011.

Conducting polymers are found to be highly attractive among researchers because of their unique electronic, magnetic and optical properties. The nano composite form of conducting polymers has attracted special attention for their universal applications in drug delivery systems, plastic transistors, and in microwave components after coating metal, electronic, and electro optical devices. These types of organic polymers have been shown to be excellent hosts for trapping nano particles of metals and semiconductors because of their ability to act as stabilizers or surface capping agents.[1–7] When the nanoparticles are embedded or encapsulated in a polymer, the polymer terminates the growth of the particles by controlling the nucleation. For application in electronics the control of particle size and their uniform distribution within the polymer is the key to technology. Among the conducting polymers, polyaniline (PANI) is one of the most studied electrically conducting polymers because of its good processibility, environmental stability, and potential in the catalyst field, biosensors, batteries and electronic technology.[8]

Heterogeneous-conducting polymer nanocomposites, especially for organic/inorganic nanocomposites, have drawn the attention of scientists over the last few years.[9] The most studied composites are polyaniline-widly $BaTiO_3$ composite,[10] polyaniline-molybdenum trisulfide composites[11] polyaniline-inorganic salt composite[12] and polyaniline–V_2O_5 composite.[13]

There are variety of attempts to achieve polymer grafted nano-sized silica composites,[14] several inorganic nanoparticles such as CdS and Cu_2S,[15] clay,[16] magnetite,[17] MnO_2,[18] TiO_2,[19] and ZrO_2.[20] Conductive PANI-metal nano composites such as [21] gold, silver and titanium provide a very exciting research field because of their excellent physical and chemical properties. Therefore the composite of PANI with inorganic nano particles have potential uses in technological applications. Among them, TiO_2 nano particles are appealing because of their excellent physical and chemical properties as well as extensive use in many areas, such as coatings, solar cells, and photo catalysis.[22–24] There have been many efforts toward the PANI-TiO_2 nano particles synthesized by in situ polymerization, ultrasonic irradiation, and sol-gel methods.

In the present work, we have illustrated the synthesis of polyaniline- nano TiO_2 (Rutile) composites on mild steel electrodes from aqueous oxalic acid solution by using cyclic voltammetry technique. Smooth and adherent coatings have been obtained. The protective performance of these coatings against corrosion was evaluated by using electrochemical impedance spectroscopy (EIS) and tafel polarisation in 1 % NaCl solution.

Experimental

A solartron 1280B potentiostat/galvanostat was used in the cyclic voltammetry (CV) studies. A conventional three-electrode system was employed during the electrosynthesis and corrosion experiments. In all cases, the working electrode was a piece of mild steel containing (in wt %) C (0.10), Mn (0.45), S (0.035) and P (0.06) with 1 cm^2 surface area. Large area Pt was employed as counter electrode. All potentials were measured against a saturated calomel electrode (SCE). Cyclic voltammetry experiments were carried out by scanning the potential of working electrode from −0.5 to 1.6 V vs SCE at a scan rate of 10 mV s^{-1}. An aqueous bath containing 0.3 M oxalic acid, 0.1 M aniline and 0.01 M nano TiO_2 (Rutile) was used for PANI-nano TiO_2 composite coating formation. During electropolymerisation, the solution was constantly stirred so as to keep the nano TiO_2 particles in dispersed state. Before each experiment, the working electrode was polished with emery paper (1200 grit) and finally rinsed with distilled water.

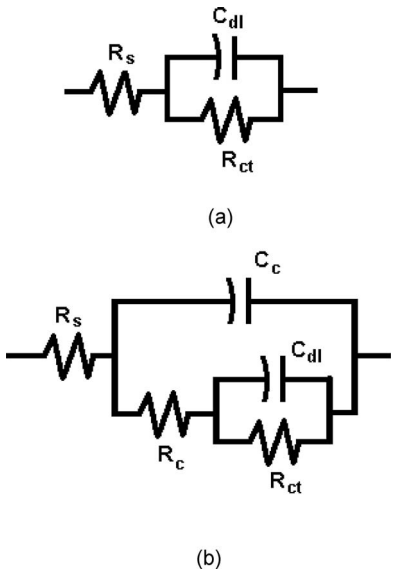

Figure 1. (a) Equivalent circuit for uncoated steel (b) Equivalent circuit for coated steel.

[z] E-mail: sathya_cecri@yahoo.co.in

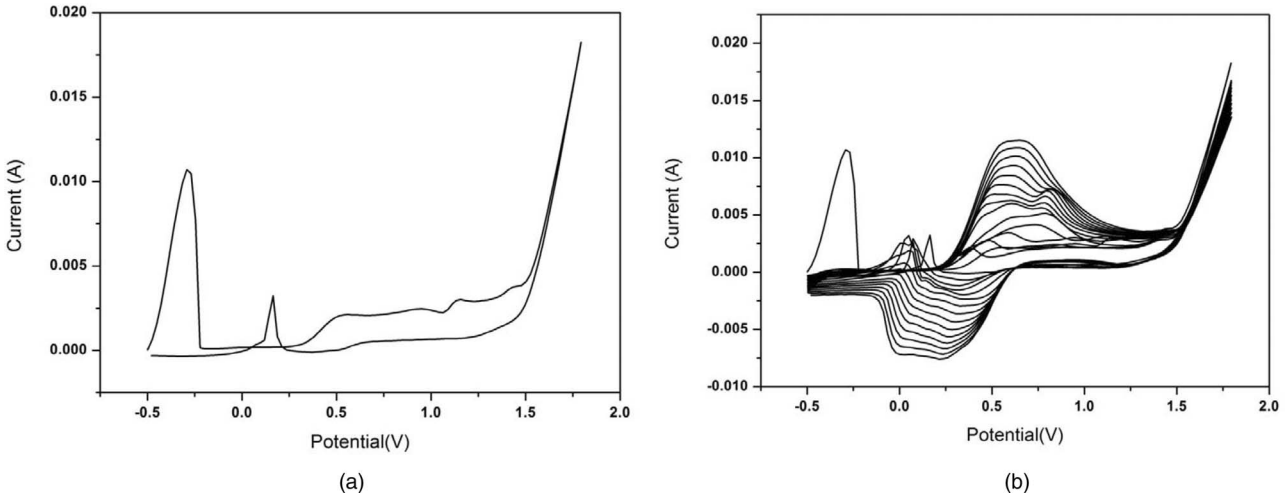

Figure 2. (a) First cycle CV of Electro synthesized polyaniline on steel (b) Electro synthesis of PANI on steel.

Characterization.—FTIR Spectroscopy.— The electrosynthesized PANI-TiO_2 coating over steel was characterized using Nicolet 380 FTIR instrument having ATR attachment.

Morphology studies.— The morphology of the electrosynthesized PANI-TiO_2 coating was analysed using Hitachi (Model s3000H) Scanning electron microscopy and EDX analysis were performed using a Philps XL 30 instrument.

XPS studies.— X-ray photoelectron spectra (XPS) of the steel sample with PANI-TiO_2 polymer coating were recorded on Multilab 2000 (Thermofisher scientific, UK) fitted with a twin anode X-ray source using MgKα radiation (1253.6 eV). The sample was mounted on the stainless steel sample stubs using conducting silver paint (Agar scientific Ltd, UK). The stub was initially kept in the preparatory chamber overnight for desorbing any volatile species at 10^{-9} mbar was introduced into the analysis chamber having a base pressure of 9.8 $\times 10^{-10}$ mbar for recording positive spectra. High-resolution spectra averaged over 5 scans with dwell time of 100 ms in steps of 0.05 eV obtained at pass energy of 20 eV in constant analyzer energy mode. The binding energy was referenced with C (1 s) at 284.98 eV with an accuracy of ± 0.05 eV.

Corrosion resistance property evaluation.— The electrosynthesized polyaniline and polyaniline-nanoTiO_2 composite (PnTC) coatings were evaluated for their corrosion resistance property in 1 % NaCl by electrochemical impedance spectroscopy (EIS) and Tafel polarization.

In the case of electrochemical impedance spectroscopy, a.c signals of 20 mV amplitude and various frequencies from 10 kHz to 0.1Hz were impressed to the coated steel at open circuit potential. The results were analyzed in the Nyquist format using the Z view software. Since the Nyquist curves show single semi circle in the case of uncoated steel, the semicircular fit was made and the charge transfer resistance (R_{ct}) and the double layer capacitance (C_{dl}) values were obtained by analyzing the data using the Randles equivalent circuit (Fig. 1a). In the case of coated steel, the equivalent circuit consisting of two time constants (Fig. 1b) was used in which R_c and C_c represents coating resistance and coating capacitance respectively.

From the measured charge transfer resistance values, the protection efficiency (PE) of the coating has been obtained from the relationship.

$$PE(\%) = \frac{R^*_{ct} - R_{ct}}{R^*_{ct}} \times 100$$

where R^*_{ct} and R_{ct} are the charge transfer resistance values in the presence and absence of coating.

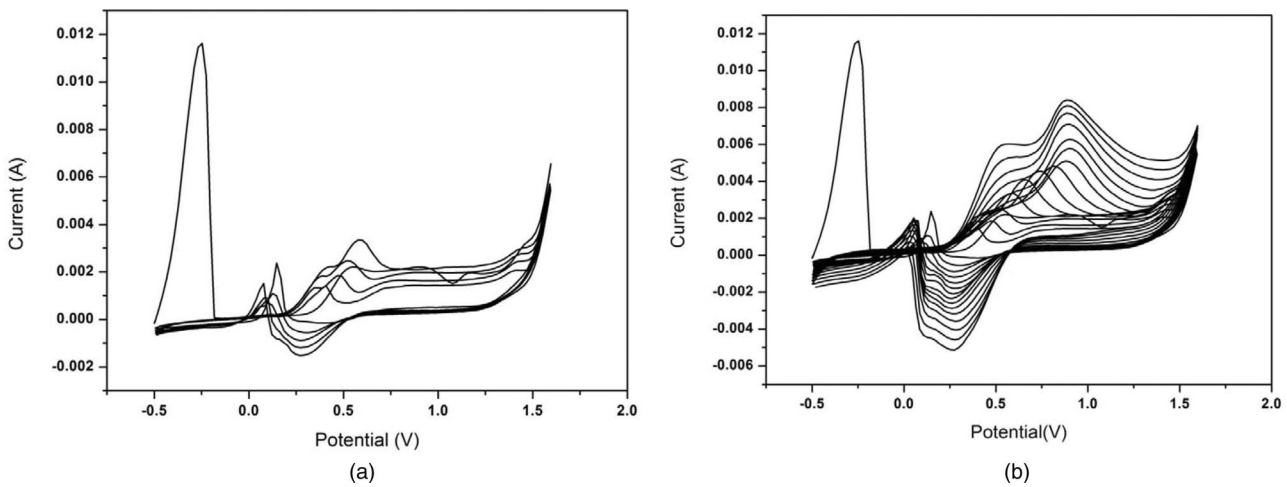

Figure 3. (a) Electrosynthesis of PANI- nano TiO_2 coating on steel by cyclic voltammetry (First 5 cycles) (b) Electrosynthesis of PANI-nano TiO_2 coating on steel by cyclic voltammetry.

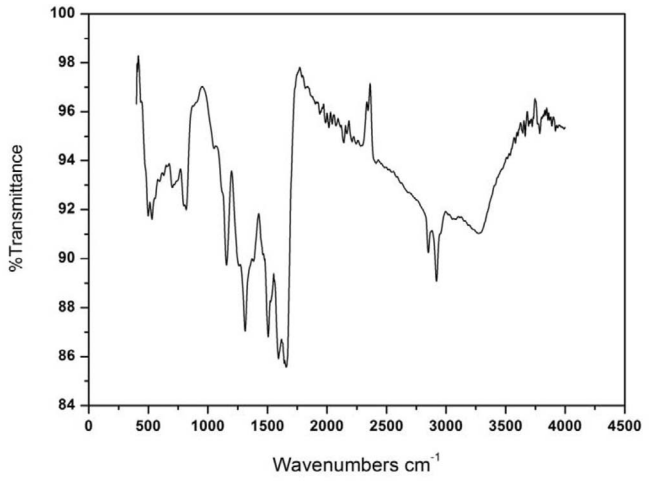

Figure 4. FTIR spectrum of PANI coating.

In the case of Tafel polarization, the potential of the working electrode was scanned from −0.2 V to + 0.2 V vs open circuit potential (OCP) at the scan rate of 1 mv/sec using Corrware software. From the anodic and cathodic polarization curves, the Tafel regions were identified and extrapolated to corrosion potential (E_{corr}) to get corrosion current (i_{corr}) by using the auto tafel fit feature of Corrview software. From the corrosion current values, the protection efficiencies were obtained from

$$PE(\%) = \frac{i_{corr} - i^*_{corr}}{i_{corr}} \times 100$$

where i_{Corr} and i^*_{Corr} are the corrosion current values in the absence and presence of the coating.

Results and Discussion

Electrosynthesis of poly (aniline-nano TiO_2 composite).— The electropolymerization of aniline in 0.3 M oxalic acid solution was carried out by sweeping the potential between −0.5 and +1.6 V vs SCE at a scan rate of 10 mV s^{-1}. In the first scan, as shown in Fig 2a, an oxidation wave appears starting at about −0.5 V vs SCE, which corresponds to the dissolution of iron and then a weak wave after about +0.5 V vs SCE which is attributed to the oxidation of Fe^{2+} ions produced during the dissolution interact with the oxalate electrolyte to form insloluble iron(II) oxlate film which adhers to the electrode surface. The dissolution peak of iron appears only during the first positive scan and disappears completely in subsequent scans [Fig 2b] and beyond −0.3 V vs SCE, the steel electrode is passivated.[25–28] This layer isolates the electrode surface and the metal behaves like an inert metal. More soluble iron(III) oxalate is also formed during this initial positive scan which created micropores in the insoluble iron(II) oxalate film and oxidation of the underlying iron to iron (III) oxide has occurred within these pores.[28] During the first reverse sweep, a sharp oxidation current appears at about −0.10 V(repassivation peak).[26,28] This sharp peak correponds to the restoration of the iron (II) oxalate passive film from iron (III) species which were formed during the initial positive sweep.[29,30] The intensity of the repassivation peak gradually decreases with subsequent scans.

After the initial oxidation of the monomer, the oxidation and reduction peaks of PANI appear after the first scan, indicating the growth of the polymer layer (Fig 2b). This indicates the buildup of an electroactive polymeric material on the steel surface. The CV curves recorded for PANI-TiO_2 coating formation for 5th & 15th cycles are shown in Figs 3a & 3b. There is a broad oxidation and reduction peak which indicates the redox property of nano-TiO_2 incoporated PANI. Increase in the peak current of peaks show that the deposition thickness increases with cycles.The thickness of the

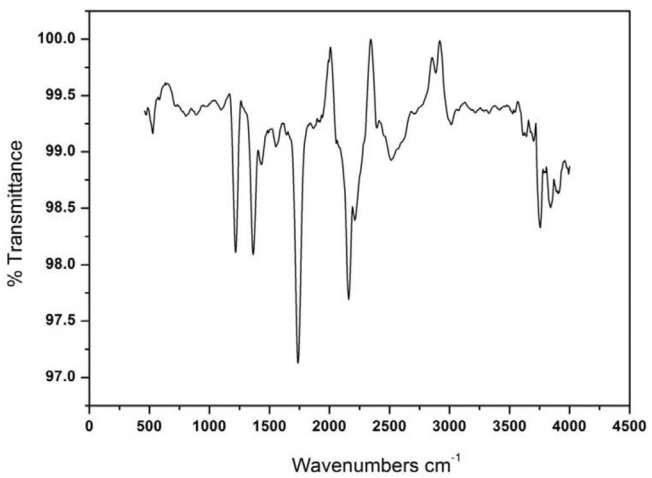

Figure 5. FTIR spectrum for PANI- nano TiO_2 coating.

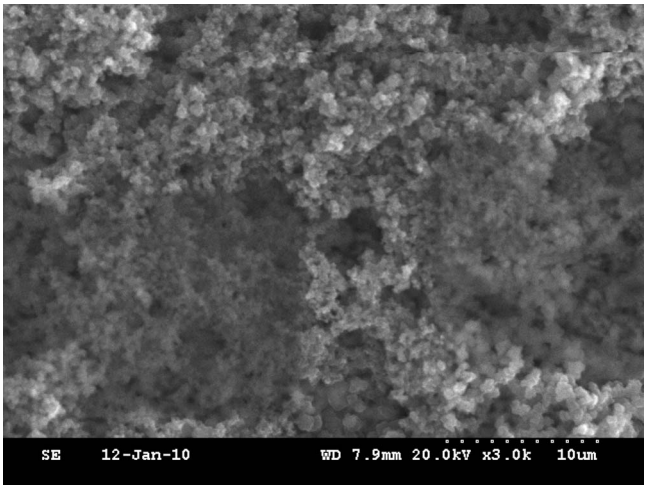

Figure 6. SEM micrograph of PANI coating on steel.

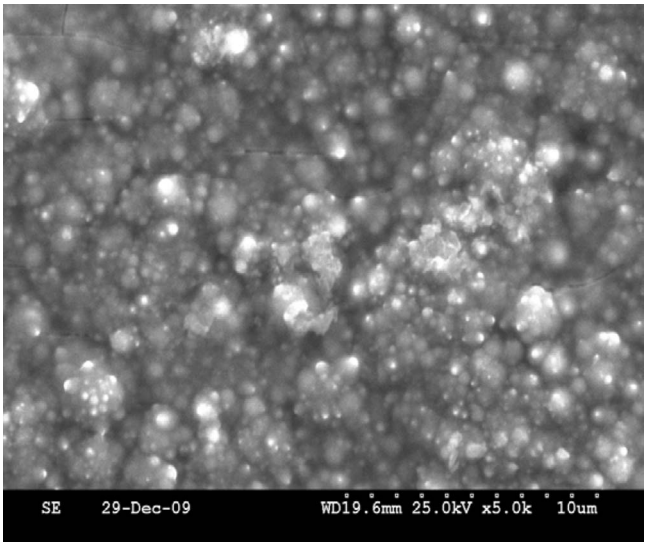

Figure 7. SEM micrographs of PANI- nano TiO_2 coating on steel.

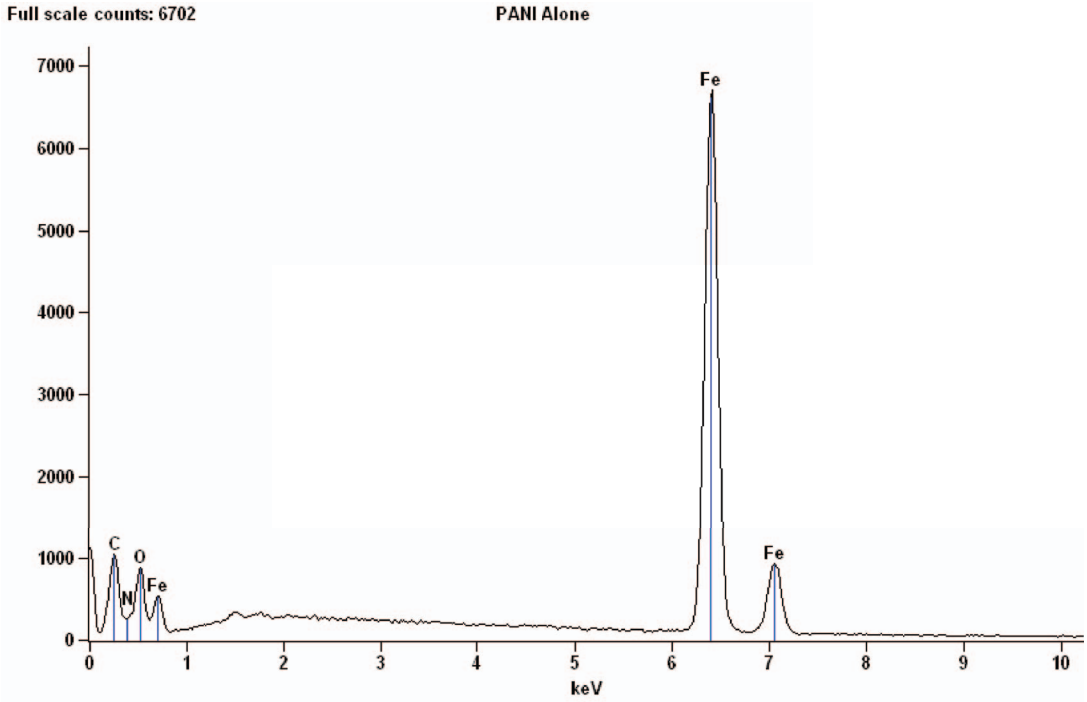

Quantitative EDAX results of PANI coating on steel

Element	Net Counts	Weight %	Atom %
C	9348	37.09	62.66
N	813	5.02	7.28
O	6901	9.97	12.65
Fe	117304	47.92	17.41
Total		100.00	100.00

Figure 8. EDAX analysis of PANI coated steel.

electrosynthesized polyaniline-nano TiO_2 composite coating on steel was measured using Elcometer. After 15 cycles it was found to be 78 ± 5 μm.

FTIR spectroscopy.— The FTIR spectra of the PANI and PANI-nanoTiO_2 composite coatings are shown in Figs 4 and 5. The PANI spectra (Fig. 4) is in correlation with previously reported results.[5,31–33] The bands at 1592 and 1570 cm^{-1} show the characteristic C=C stretching of the quinoid and benzenoid rings. The peaks at 1313 and 817 cm^{-1} can be assigned to the C-N stretching of the secondary aromatic amine and an aromatic C-H out-of-plane bending vibration respectively.The relatively small peak at

Table I. Corrosion protection performance of electrosynthesized polyaniline coating on steel in 1 % NaCl.

	Impedance					Tafel polarization		
Number of cycles	Coating capacitance C_c (F/cm^2)	Coating resistance R_c Ω,cm^2	Double layer capacitance C_{dl} (F/cm^2)	Charge transfer resistance R_{ct} Ω,cm^2	Protection efficiency (%)	E_{corr} mV vs SCE	i_{corr} (μA/ cm^2)	Protection efficiency (%)
Blank	–	–	1.863×10^{-4}	27	–	−0.701	114	–
5	3.76×10^{-8}	11	5.626×10^{-3}	150	81	−0.692	18	84
10	1.83×10^{-8}	15	8.186×10^{-3}	164	83	−0.653	14	87
15	3.42×10^{-7}	22	7.671×10^{-4}	245	88	−0.644	13	88

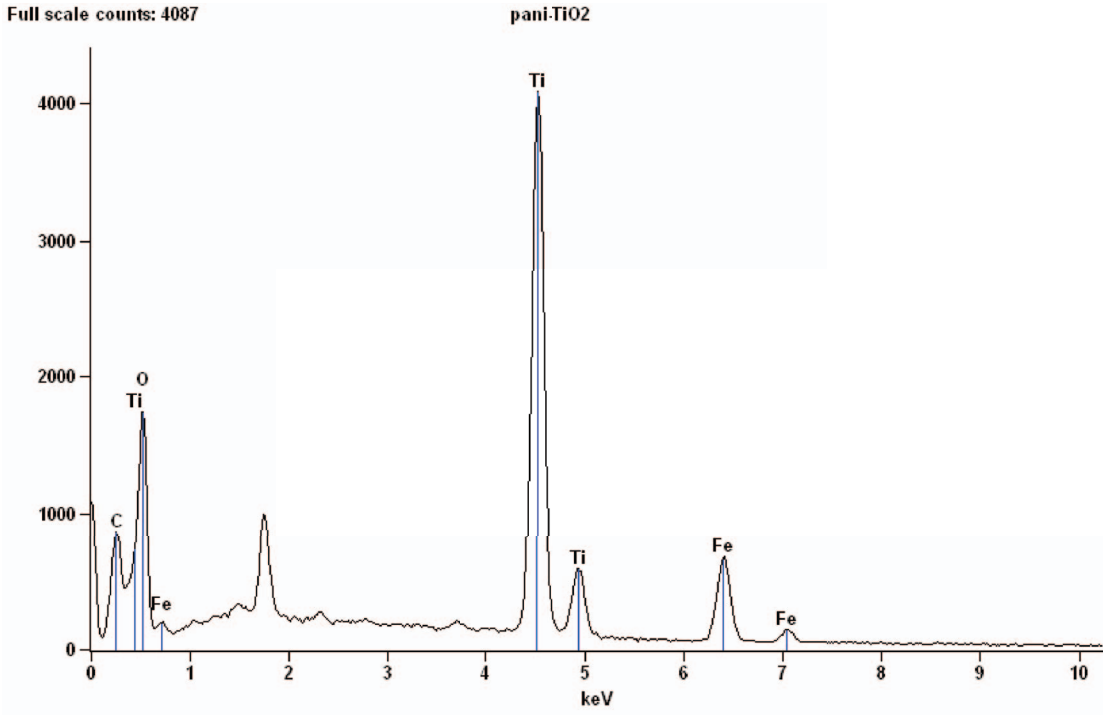

Quantitative EDAX results of PANI-nanoTiO$_2$ coating on steel

Element	*Net Counts*	*Weight %*	*Atom %*
C	8851	32.78	47.30
O	16081	39.75	43.06
Ti	62241	21.53	7.79
Fe	10742	5.93	1.84
Total		100.00	100.00

Figure 9. EDAX analysis of PANI – nano TiO_2 coated steel.

3271 cm^{-1} can be attributed to the N-H stretching mode.In the region of 1000–1170 cm^{-1}, aromatic C-H in-plane bending modes are usually observed.[34]

The FTIR spectra of PANI – TiO_2 (Fig. 5) indicate all characteristic bands of PANI present between 700 and 1600 cm^{-1}. The relative intensity of some bands have changed due to presence of nano-TiO_2, and the presence of TiO_2 nano particles led to the shift of some peaks of PANI macromolecules. For example, the peaks at 1506 and 1313 cm^{-1} shift to 1494 and 1302 cm^{-1} respectively and the peak associated with the doping of PANI also shifts from 1155 cm^{-1} to 1140 cm^{-1}. Moreover, higher bands at 3271 cm^{-1} for the N-H stretching of PANI is not present in the PANI – TiO_2 composite. This is probably due to the formation of hydrogen bonding between the surfaces of the TiO_2 nano particles and the N-H groups in the PANI macromolecules. Besides, it is found that the ratio between quinoid and benzenoid rings is changed for PANI–TiO_2 composite. Since titanium is a

Table II. Corrosion protection performance of electro synthesized PANI – nano TiO_2 coating on steel in 1 % NaCl.

			Impedance			Tafel polarization		
Number of cycles	Coating capacitance C_c (F/cm^2)	Coating resistance R_c Ω,cm^2	Double layer capacitance C_{dl} (F/cm^2)	Charge transfer resistance R_{ct} Ω,cm^2	Protection efficiency (%)	e_{corr} mV vs SCE	i_{corr} (μA/ cm^2)	Protection efficiency (%)
Blank			1.8×10^{-4}	27	–	−0.701	114	–
5	4.65×10^{-9}	18	6.1×10^{-3}	104	74	−0.606	25	78
10	7.39×10^{-5}	85	1.3×10^{-3}	608	95	−0.687	11	90
15	2.66×10^{-4}	99	8.0×10^{-4}	1231	97	−0.605	4.2	96

transition metal, titania has an intense tendency to form co-ordianation compound with nitrogen atom in PANI macromolecule.[35]

These two types of bonding decrease the force constant between atoms and cause the absorption peaks to move to lower wavenumbers. Further in the case of PANI – TiO_2 coating, strong absorption around 670 cm^{-1} for TiO_2 does not appear which is due to the uniform coverage of PANI on TiO_2.[36]

SEM analysis.— Scanning electron microscopic images of PANI and PANI-TiO_2 nano composites are displayed in Figs 6 and 7 respectively. From Fig 6 one can see that the PANI synthesized without TiO_2 nanoparticles shows non homogenous morphology. Fig 7 shows that the coating is homogenous and the PANI-TiO_2 nano sized composites with the diameter between 50 and 200 nm are produced by the electro polymerization method. EDAX analysis of PANI (Fig. 8) and PANI-nanoTiO_2 composite coating (Fig. 9) indicates the presence of various elements present in the coating. Besides, it is found that PANI – TiO_2 coating is relatively more homogenous and less porous which is evidenced from the lower iron count.

XPS analysis.— In the XPS spectra of the PANI–TiO_2 nano composite (Fig. 10) the elements C,O,Ti and N are detected with binding energies of 284,529,458, and 400 eV respectively. This result implies that TiO_2 nanoparticles are trapped in the PANI matrix in the process of polymerization. The O 1s signal at 529 eV confirms the presence of Ti-O bond in TiO_2. The binding energy (400 eV) of N1 s in the nano composite, which is higher than that of PANI,[40] also indicates that there is a strong interaction (eg. Hydrogen bonding) between TiO_2 and PANI.

Corrosion protection evaluation.— The corrosion behaviour of PANI and PANI- nanoTiO_2 coated steel in 1 % NaCl has been studied by EIS and polarization methods. Fig. 11 shows the Nyquist representation of impedance behaviour of PANI coated steel by 5, 10, and 15 cycles of deposition in 1 % NaCl and the impedance parameters such as Coating resistance ($R_{c,}$), Coating capacitance (C_c), Charge transfer resistance (R_{ct}) and Double layer capacitance (C_{dl}) obtained from these curves are given in Table I. The charge transfer resistance is increased from 27 $\Omega.cm^2$ for the case of PANI free steel surface to 150 Ω $.cm^2$ and 245 Ω. cm^2 respectively for 10 and 15 cycles of PANI deposited steel surface. Besides the C_{dl} values are found to be increased by several folds due to the coverage of iron surface with conducting PANI. Similar behaviour is observed in polarization studies as shown in Fig 12. The corrosion kinetic data obtained from these curves are also included in Table I. The corrosion current density is decreased to 18 $\mu A/cm^2$ for PANI coated steel at 5 cycles from 114 $\mu A/cm^2$ corresponding to that of PANI free steel surface. With increase in potential cycling, the i_{corr} values are decreased and after 15 cycles, the coating offers nearly 88 % corrosion protection. The impedance and polarization behaviour of PANI-nano TiO_2 composite coated steel in 1 % NaCl are shown in Figs 13 and 14 and the parameters obtained from these figures are given in Table II. In the case of 5 cycles of deposition, the protection efficiency of PANI-nano TiO_2 is less than that of pure PANI coating. This may be due to the fact that the adsorption of nano TiO_2 particles on PANI – steel surface might have caused some heterogeneity which is probably due to the difference in size of nano TiO_2 and thickness of deposited PANI film. With increase in number of potential cycling viz 10 cycles, the R_{ct} value is increased considerably and showed a protection efficiency of 97 %. The i_{corr} values also indicate a higher protection efficiency in comparison with pure PANI coating. Besides, the coating resistance (R_c) values of PANI-TiO_2 composite is found to be more in comparison with that of PANI coating. This indicates that the PANI-TiO_2 composite coating is more compact than that of PANI coating. Since nano-TiO_2 particles act as anchoring sites during the formation of PANI coating, denser and homogenous coating is formed.

In general, TiO_2 particles are electronegative in aqueous acidic solution and the anilinium cations might have a possibility to get adsorbed on the surface of TiO_2 nano particles due to electrostatic attraction. As per nucleation and growth theory, nano particles are intrinsically produced in the initial stage of polymerization.[37] As a result, free aniline cation-radicals adsorb on the surface of TiO_2 nanoparticles growing together during the electro polymerization and produce coatings of denser and more compact morphology.[38,39] The dense and

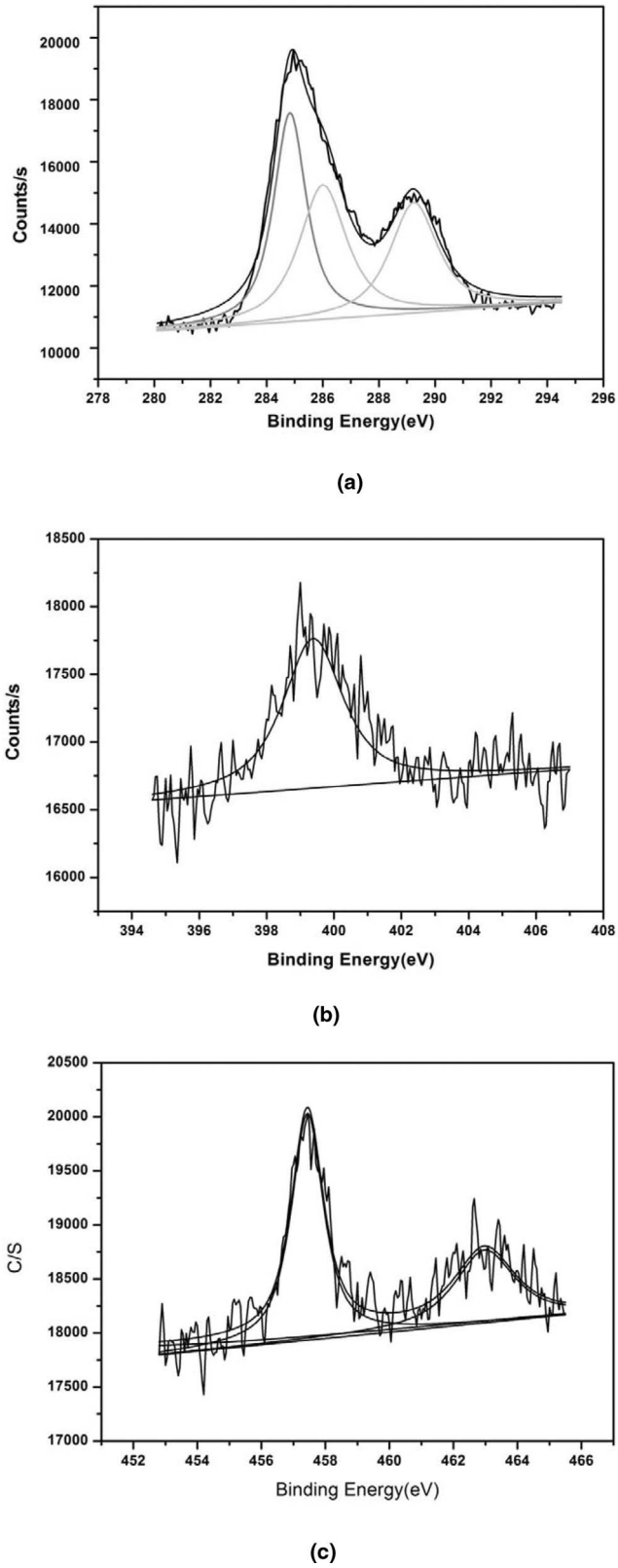

Figure 10. XPS Survey spectra of PANI- nano TiO_2 coated steel.

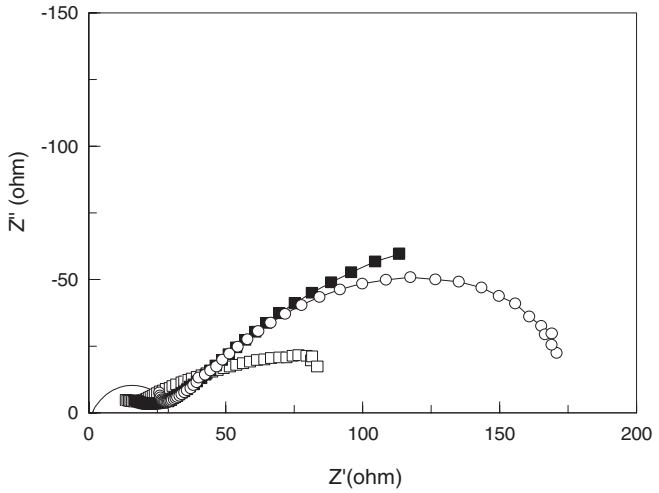

Figure 11. Impedance behavior of electropolymersied polyaniline on steel in1 % NaCl—Blank □ 5cycles:■ 10 cycles ○ 15 cycles.

compact PANI-TiO_2 composite coating at the metal-solution interface forms a highly protective passive layer due to redox property of the conducting polymer. The formation of more protective passive layer in the case of PANI-nanoTiO_2 composite coating than that of PANI coating is evidenced from the shift in open circuit potential values (OCP) to more noble direction for PANI-nanoTiO_2 composite coating.

Stability of the PANI-nano TiO_2 composite coating on steel.— In order to obtain further knowledge about electrochemical properties and stability of the PANI-nano TiO_2 composite coating on steel, cyclic voltammetry was run in monomer free 0.3 M oxalic acid solutions with PANI and PANI – nano TiO_2 covered steel surface as working electrodes (Figs. 15 & 16) respectively. The figure exhibits redox property of PANI- nanoTiO_2 composite film through its oxidation and reduction peak. It is well known that PANI undergoes electrochemical degradation by application of sufficiently high anodic potential.[41] Though the current peaks in the cyclic voltammogram of composite film diminish in height during prolonged potential cycling it is found that the PANI-TiO_2 composite film withstands up to 50 cycles which lead to the conclusion that the electrosynthesized polyaniline nano TiO_2 composite exhibits relatively better stable electro activity.[42]

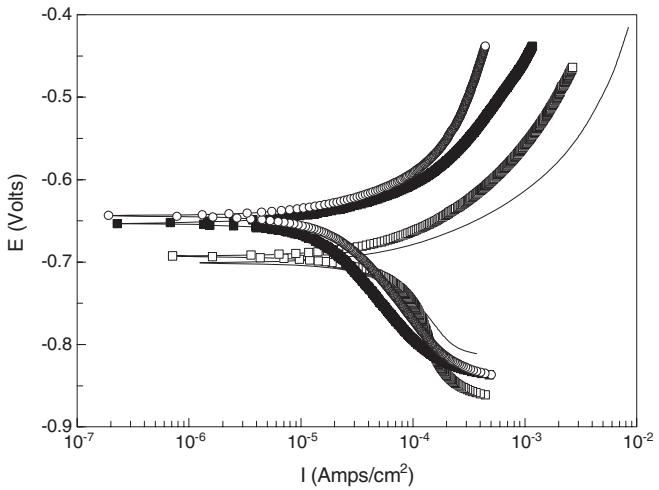

Figure 12. Polarization behavior of electropolymersied polyaniline coated steel in 1 % NaCl—Blank □ 5 cycles:■ 10 cycles ○ 15 cycle.

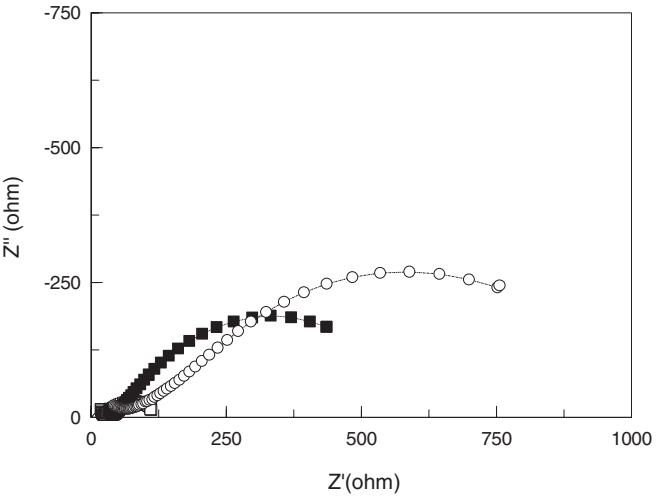

Figure 13. Impedance behavior of electropolymersied polyaniline- nano TiO_2 Composite coating on steel in1 % NaCl—Blank □ 5 cycles:■ 10 cycles ○ 15 cycles.

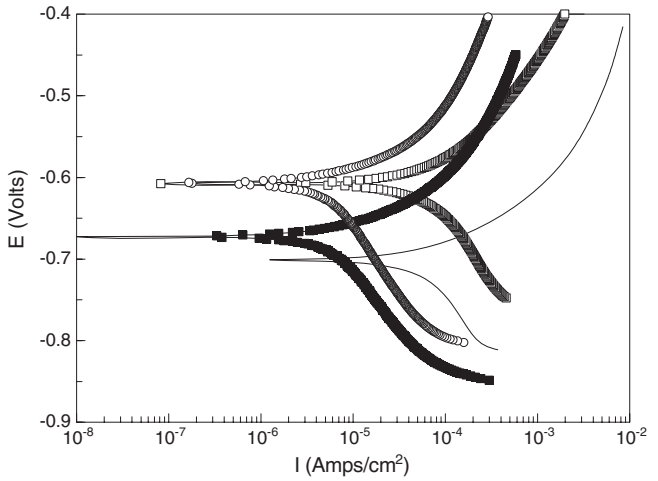

Figure 14. Polarization behavior of electropolymersied polyaniline-nano TiO_2 Composite coating on steel % NaCl—Blank □ 5 cycles ■ 10 cycles ○ 15 cycles.

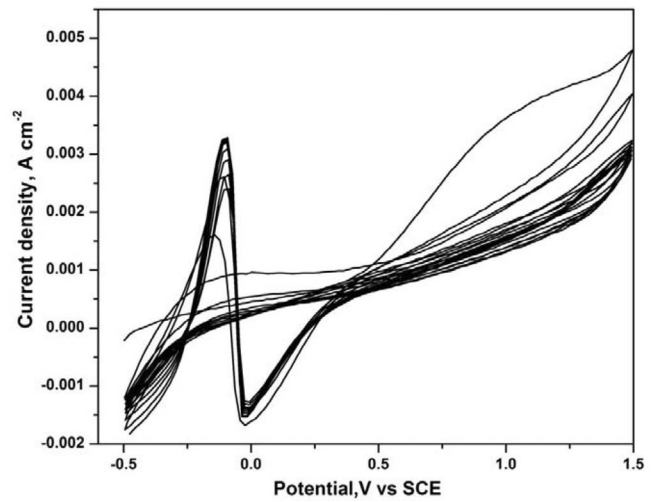

Figure 15. Cyclic voltammogram of electrosynthesized polyaniline coating on steel in monomer free 0.3 M oxalic acid solution.

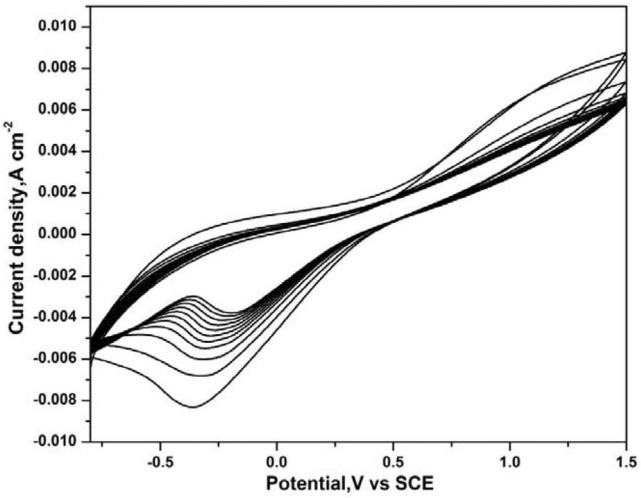

Figure 16. Cyclic voltammogram of electrosynthesized polyaniline nanoTiO_2 composite coating on steel in monomer free 0.3 M oxalic acid solution.

Conclusion

Highly adherent PANI-nanoTiO_2 composite coatings on steel can be formed by electro polymerization of aniline in the presence of nano TiO_2. The composite film is mainly composed of TiO_2 core encapsulated by PANI which is evidenced from the FTIR study. The PANI-nano TiO_2 composite coating has more corrosion resistance on steel compared to that of pure PANI coating due to the formation of denser and homogenous compact film.

Acknowledgment

The authors thank The Director, Central Electrochemical Research Institute, Karaikudi-6 for his keen support and encouragement. They also thank CSIR, New Delhi for financial support under NWP – 12 project. One of the authors (K.K) thanks CSIR, New Delhi for the financial support through Senior Research Fellowship.

References

1. M. R. Karim, C. J Lee, A. M. S. Chowdhry, N. Nahar, and M. S Lee, *Mater.Lett.*, **61**, 1688–1692 (2007).
2. M. R Karim, C. J. Lee, and M. S Lee, *Polym.Chem.*, **44**, 5283–5290 (2006).
3. Z. Zhang and M. Hang, *J. Mater. Chem.Commun.*, **13**, 641–643 (2003).
4. P. K. Khanna, S Lonkar, V. S Subbarao, and K. -W Jun, *Mater.Chem.Phys.*, **87**, 49–52 (2004).
5. D. W DeBerry, *J. Electrochem. Soc.*, **132**, 1022–1026 (1985).
6. G. Mengoli, *J.Appl.Polym.Sci*, **26**, 4247–4257 (1981).
7. M. R. Karim, C. J. Lee, Y. T Park, and M. S. Lee, *Synth. Met.*, **151**, 131–135 (2005).
8. C. G Wu, C. DeGroot, Ho Marcy, J. L. Schindler, C. R. Kannewurf, and Y. J. Liu, *Chem. Mater*, **8**, 1992–2004 (1996).
9. P. Somani, B. B. Kale, and D. P. Amalnerkar, *Synth. Met.*, **106**, 53–61 (1999).
10. F. Fusalba and DJ Belganger, *J.Mater. Res.*, **14**, 1805–1818 (1999).
11. I. Krivka, J. Prokes, and E. Tobolkova, and J. Stejskal, *J. Mater. Chem.*, **9**, 2425–2433 (1999).
12. Lira-Gantu and P. J. Gomez-Romero, *J.Solid State. Chem.*, **147**, 601–609 (1999).
13. K. Yoshinaga, *Bull. Chem.Soc.Jpn.*, **75**, 2349–2358 (2002).
14. R. L. N. Chandrakanthi and M. A. Careem, *Thin Solid Filims.*, **417**, 51–56 (2002).
15. G. M. doNascimento, V. R. L. Constantino, and M. L. A. Temperini, *Macromolecules.*, **35**, 7535–7537 (2002).
16. B. Z. Tang, Y. H Geng, J. W. Y. Lam, amd B. S. Li, *Chem.Mater.*, **11**, 1581–1589 (1999).
17. M. Biswas, S. S. Ray, and Y. P Liu, *Synth.Met.*, **105**, 99–105 (1999).
18. S. J Su and N. Kuramoto, *Synth.Met*, **114**, 147–150 (2000).
19. S. S Ray and M. Biswas, *Synth.Met*, **108**, 231–236 (2000).
20. R. Gangopadhyay and A. De, *Chem.Mater*, **12**, 608–622 (2000).
21. S. Roux, P. Audebert, and C. Sanchez, *Adv.Mater*, **15**, 217–238 (2003).
22. D. Chowdhury, A. Palu, and A. Chattopadhyay, *Langmuir.*, **21**, 4123–4128 (2005).
23. M. K Norimoto, T. watanabe, K. Hashimoto, and A. Fujishima, *J.Mater.Sci.*, **34**, 2569–2574 (1999).
24. W. Feng, E. Sun, A. Fujii, H. C. wu, K. Niihara, and K. Yoshino, *Bull. Chem.Soc.Jpn.*, **73**, 2627–2633 (2000).
25. L. J. Zhang and M. X Wan, *J. Phys.Chem. B.*, **107**, 6748–6753 (2003).
26. C. Bian, Y. Yu, and G Xue, *J. Appl.Polym.Sci.*, **104**, 21–26 (2007).
27. H. S Xia and Q. Wang, *Chem, Mater.*, **14**, 2158–2165 (2002).
28. A. Yagan,N. O. Pekmez, and A. Yildiz, *J. Electroanal.chem*, **578**, 231 (2005).
29. G. Mengoli and M M Musiani, *Electrochim.Acta.*, **31**, 201–210 (1986).
30. M. G. Wankhede, P. M. Koinkar, M. A. More, P. P Patil, and S. A. Gangal, *Mater Sci.Eng A.*, **347**, 365–373 (2003).
31. K. Shah, *J. Synth.Met.*, **132**, 35–41 (2002).
32. H. K. Chaudhari and D. S Kelkar, *Polym.Int.*, **42**, 380–384 (1997).
33. H. Liu, X. B. Hu, J. Y Wang, and R. I. Boughton, *Macromolecules.*, **35**, 9414–9419 (2002).
34. M. R Karim, C. J Lee, and M. S Lee, *J.Appl.Polym.Sci.*, **103**, 1973–1977 (2007).
35. X. W Li, W Chen, C. Q Bian, J. B He, and N. Xu, *Appl.Surf.Sci.*, **217**, 16–22 (2003).
36. K Gurunathan, D. P Amalnerkar, and D. C Trivedi, *Mater.Lett.*, **57**, 1642–1645 (2003).
37. N. R. Chiou and A. J. Epstein, *Synth. Met*, **153**, 69–72 (2005).
38. Y. C. Liu and B. J. Hwang, *Thin. Solid. Films.*, **360**, 1–9 (2000).
39. K. G Neoh, T. T. Young, E. T Kang, and K. L. Tan, *J.Appl.Poly.Sci.*, **66**, 519–526 (1997).
40. C. G Wu and J. Y Chen, *Chem. Mater.*, **9**, 399–402 (1997).
41. T. Kobayashi, H. Yoneyama, and H. Tamura, *J. Electroanal. Chem.*, **177**, 293 (1984).
42. M. Nakayama, S. Saeki, and K. Ogura, *Anal. Sci.*, **15**, 259 (1999).